Brazilian Journal
of Chemical
Engineering

ISSN 0104-6632
Printed in Brazil
www.abeq.org.br/bjche

Vol. 32, No. 03, pp. 671 - 682, July - September, 2015
dx.doi.org/10.1590/0104-6632.20150323s00003444

DENSITY, REFRACTIVE INDEX, APPARENT VOLUMES AND EXCESS MOLAR VOLUMES OF FOUR PROTIC IONIC LIQUIDS + WATER AT T=298.15 AND 323.15 K

R. Rocha Pinto[1*], D. Santos[2], S. Mattedi[2] and M. Aznar[1†]

[1]School of Chemical Engineering, University of Campinas (UNICAMP),
Av. Albert Einstein 500, Cidade Universitária, 13083-852, Campinas - SP, Brazil.
Phone: + (55) (19) 3521-3962
E-mail: rafarocha@feq.unicamp.br
[2]Department of Chemical Engineering, Federal University of Bahia (UFBA),
R. Aristides Novis 2, Federação, 40210-630, Salvador - BA, Brazil.
Phone: + (55) (71) 3282-9801

(Submitted: April 14, 2014 ; Revised: October 30, 2014 ; Accepted: December 15, 2014)

Abstract - Densities and refractive index of binay mixtures of water with four protic ionic liquids, based on ammonium and fatty acids, were measured at 298.15 and 323.15 K, under atmospheric pressure. Apparent and excess molar volumes were obtained by experiments and fitting data to the Redlich-Meyer (RM), Redlich-Kister (RK) and Prigogine-Flory–Patterson (PFP) equations. The molar volume values were high, suggesting strong ion-solvent interaction. The same interaction also became stronger as the temperature increased. Excess volume values were negative, indicating that packing efficiency ability or attractive interactions occurred in mixtures of ionic liquid + water. The errors (AARD) for the properties in excess were in the range of 1.8% to 7.2%. The PFP error for the apparent volume was in the range of 0.34% to 0.06%, lower than the RM error for the same property, which was in the range of 0.70 to 1.55%. The Gladstone-Dale model was applied to correlate the refractive index of the binary mixture with the density from the values of both pure components.
Keyword: Protic ionic liquid; Water; Properties of mixtures.

INTRODUCTION

Room temperature ionic liquids form a class of organic salts that are normally liquids at temperatures below 373.15 K. They are also called designer solvents due the huge range of possible combinations of organic cations and organic or inorganic anions. This new class of materials has attracted interest as substitutes to traditional solvents due to their potential applications and low vapor pressure (Iglesias *et al*., 2010; Alvarez *et al*., 2010a; Taib *et al*., 2012).

Ionic liquids based on the imidazolium cation are the most studied and their applications are much discussed. In the last decade, protic ionic liquids began to attract more interest because they have advantageous characteristics over aprotic ionic liquids. Some works comment its simple synthesis and relevance in important processes (Bicak, 2004; Cota *et al*., 2007; Iglesias *et al*., 2010; Alvarez *et al*., 2010a). For example, ionic liquids derived from ammonium are relatively new and have a high potential for absorbing gases. When mixed with other solvents, their properties change, which can be beneficial to future processes such as gas absorption (Kurnia and Mutalib, 2011). The local structure depends on forces between molecules, shapes, volume and can change with

*To whom correspondence should be addressed
†*In Memoriam*
This is an extended version of the manuscript presented at the
VII Brazilian Congress of Applied Thermodynamics - CBTermo 2013, Uberlândia, Brazil.

composition. Besides, ionic liquids present a high hygroscopic characteristic, demonstrating the necessity to study their behavior and thermophysical properties when mixed with water.

Volume changes observed in real systems are the result of changes in solution packing of the solution and intermolecular interactions in the system. Volume changes of mixtures can be used as a parameter to assess how a particular system deviates from ideality at constant temperature and pressure. The concept of partial molar property is very important in the study of solutions, since it reflects the variation of a particular property with the composition. A partial molar quantity is the contribution (per mole) that the substance makes to some mixture property. Composition variations lead to changes in the thermodynamic properties of mixtures (Patil *et al*., 2011). Thus, in order to develop ionic liquids applications, it is essential to determine their physico-chemical properties, both as pure materials and their mixtures with traditional solvents.

In this context, the objective of this work was to synthesize four protic ionic liquids, varying the anion (butyric, pentanoic and hexanoic acid) and the cation (monoethanolamine and diethanolamine), forming 2-hydroxy ethylammonium butanoate (2-HEAB), 2-hydroxy ethylammonium pentanoate (2-HEAP), 2-hydroxy ethylammonium hexanoate (2-HEAH), and 2-hydroxy diethylammonium hexanoate (2-HDEAH). The refractive index and density of binary mixtures (2-HEAB + water, 2-HEAP + water, 2- HEAH + water and 2- HDEAH + water) were determined at 298.15 K and 323.15 K and atmospheric pressure. From the densities of binary mixtures the apparent molar volume $V_{\phi,1}$; the excess molar volume Vm^E; and the limiting apparent molar volume V_ϕ^0 were also determined. The excess functions are used to explain intermolecular interactions in these binary mixtures.

EXPERIMENTAL PROCEDURE

Materials

The reagents, monoethanolamine, diethanolamine, butanoic acid, pentanoic acid and hexanoic acid, obtained from Sigma-Aldrich, with 99% purity by mass, were used to prepare 2-hydroxy ethylammonium butanoate (2-HEAB), 2-hydroxy ethylammonium pentanoate (2-HEAP), 2-hydroxy ethylammonium hexanoate (2-HEAH) and 2-hydroxy diethylammonium hexanoate (2-HDEAH). They were produced in our laboratory, without the use of additional solvents, according to standard methods developed and reported in the literature (Bicak, 2004; Cota *et al*., 2007; Alvarez *et al*., 2010a). The protic ionic liquid synthesis method consists of treating the acid in a glass flask under magnetic stirring with base added dropwise, at aproximately 5 drops per minute. Stirring was continued for 24 h at room temperature to guarantee complete reaction. The reaction of formation of protic ionic liquids is an acid–base neutralization, producing an ester and a salt of ethanolamine. This reaction is very exothermic, so an ice bath system was used. Before each determination, the ionic liquid was purified. The purification process consists of strong agitation and slight heating, at 323.15K, for the vaporization of impurities (residual non-reacted reagents and water) under a vacuum of 20 kPa. In order to achieve humidity values below 0.1%, the liquids were submitted to this purification process for approximately 9 hours. After 6 months storage, the ionic liquids presented humidity values of nearly 10%. The humidity was verified using a volumetric Karl Fischer Titrator DL31 (Mettler Toledo). No crystallization or solidification were observed when the liquid samples were stored at 298.15 K for 6 months, and the liquids had an appearance of limpid liquid, viscous and the colors ranging from orange to yellow.

The salt formation was confirmed by the FT-IR spectrum, determined by using a Shimadzu IR Prestige 21, using a KBr disk (Cota *et al*., 2007; Iglesias *et al*., 2008; Alvarez *et al*., 2010a). Distilled water was used for the calibration of the density and refractive index instruments. Water contents in the ionic liquids were determined by a coulometric Karl Fischer titrator DL 31 (Mettler Toledo), using the CombiTitrant 5 reagent (Merck KGaA). The titrations were made in triplicate and the water content in the pure ionic liquids was less than 0.1%. The solutions were prepared by weight with a precision balance (Shimadzu model AX 200, accuracy to 0.001 g). The properties of chemicals used are listed in Table 1.

Refractive Index and Density Measurements

Binary mixtures of water + ionic liquid were prepared at various compositions and the density and refractive index were measured at 298.15 and 323.15 K. The samples were prepared in glass vials, sealed with parafilm to prevent absorption of moisture from the atmosphere, and were then stirred for 45 minutes to ensure a total molecular interaction between the compounds of the mixtures. Both experimental determinations, densities and refractive index, on all binary mixtures were made in triplicate, and the average values are considered for further analysis.

Table 1: Properties of components at 298.15 K.

Chemicals	M	ρ (g.cm^{-3})		n_D	
	g.mol^{-1}	exp	lit	exp	lit
Water	18.00	0.997043	0.99704 [a]	1.3325	1.3423 [b]
Ethylammonium	61.08	1.012301	1.01270 [c]	1.4524	1.4525 [c]
Diethylammonium	105.14	1.090198	1.09360 [c]	1.4735	1.4735 [c]
Butanoic acid	88.11	0.952644	0.95281[d]	1.3962	1.3961 [d]
Pentanoic acid	102.13	0.931426	0.93460 [e]	1.4074	1.4067 [f]
Hexanoic acid	116.16	0.921885	0.92206 [g]	1.4197	n.a.
2-hydroxy ethylammonium butanoate	149.18	1.072588	n.a.	1.4661	n.a.
2-hydroxy ethylammonium pentanoate	163.21	1.043542	1.04548 [h]	1.4645	1.4629 [h]
2-hydroxy ethylammonium hexanoate	177.24	1.019951	n.a.	1.4623	n.a.
2-hydroxy diethylammonium hexanoate	221.30	1.058710	n.a.	1.4717	n.a.

[a] Reference (Iglesias *et al*., 2010). [b] Reference (Thormahlen *et al*., 1985). [c] Reference (Murrleta-Guevara and Rodriguez, 1984).
[d] Reference (Bahadur *et al*., 2013). [e] Reference (Latcher, 2002). [f] Reference (Rubio *et al*., 2005). [g] Reference (Liao *et al*., 2012).
[h] Reference (Iglesias *et al*., 2008).

Densities of all binary mixtures were measured using an Anton Paar oscillating U-tube density meter (DMA 5000) with a measuring precision of ± 5 × 10^{-6} g.cm^{-3} at 298.15 and 323.15 K. The apparatus was calibrated frequently, by measuring the density of distilled water. The distilled water showed a density of 0.998201 g.cm^{-3} at 293.15 K, being close to the literature value (Patil *et al*., 2011; Kapadi *et al*., 2002). This apparatus yields precise results within 1 × 10^{-5} g.cm^{-3}. The uncertainty of density measurements was found to be better than ± 7 × 10^{-6} g.cm^{-3} for measuremnets at 298.15 K and ± 1 × 10^{-5} g.cm^{-3} for measurements at 323.15 K. Sample volumes used in each density determination were ca. 1.5 ml.

The refractive indices of binary mixtures (2-hydroxy ethylammonium butanoate + water; 2-hydroxy ethylammonium pentanoate + water; 2-hydroxy ethylammonium hexanoate + water and 2-hydroxy diethylammonium hexanoate + water) were measured using a Mettler Toledo RE 40D digital refractometer, with a measuring precision of ± 1 × 10^{-4}, at 298.15 and 323.15 K. The equipament was calibrated by measuring the refractive index of air and distilled water. The uncertainty of refractive index measurements was found to be better than ± 2 × 10^{-5} at 298.15 K and ± 1 × 10^{-4} at 323.15 K. Sample volumes used in each refractive index determination were ca. 0.2 ml.

RESULTS AND DISCUSSION

FT-IR Spectroscopy

The results of the FT-IR analyses were very similar for the four ionic liquids, showing the same broad bands, as can be seen in Figure 1. In special, two bands should be observed to analyze an ammonium salt formation. One band must be in the 3200–2400 cm^{-1} range, implying the typical ammonium structure. The OH stretching vibration is embedded in this band. The other important band to verify is the band centered at 1600 cm^{-1}. This is a combined band of the carbonyl stretching and N–H in-plane bending vibrations. Both bands described above can be observed in Figure 1. Similar behaviors are presented in other works (Iglesias *et al*., 2010; Cota *et al*., 2007; Iglesias *et al*., 2008; Alvarez *et al*., 2010b).

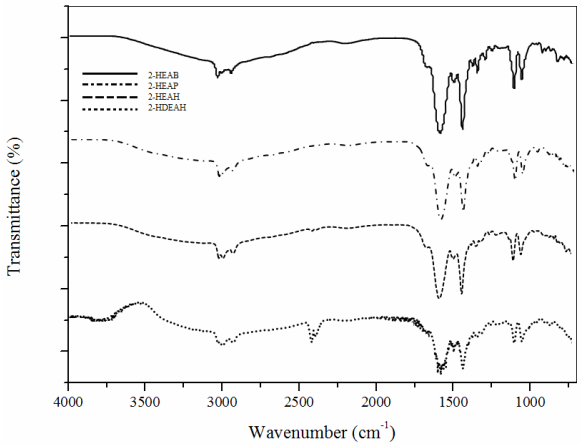

Figure 1: FT-IR spectra for 2-HEAB, 2-HEAP, 2-HEAH and 2-HDEAH.

Density and Refractive Index

Experimental data of the density ρ and refractive index n_D for binary systems (ionic liquid + water) at 298.15 and 323.15 K and atmospheric pressure are reported in Table 2, as a function of the ionic liquid mole fraction. The results in Table 2 reveal that density values for the studied mixtures increase as the concentration of the ionic liquid in water increases, achieving maximum values at 0.3255, 0.3060, 0.1937 and 0.1832 ionic liquid mole fraction of 2-HEAB, 2-HEAP,

Table 2: Mole fraction, x_1, molality, m, experimental density, ρ, refractive index, n_D, Excess Molar Volumes, Vm^E, and Apparent molar Volumes, $V_{\phi,1}$ of ionic liquids (1) + water (2).

	m/mol. kg^{-1}	ρ/g.cm^{-3}		n_D		Vm^E /cm^{-3}.mol^{-1}		$V_{\phi,1}$ /cm^{-3}.mol^{-1}	
x_1		25 °C	50 °C	25 °C	50 °C	25 °C	50 °C	25 °C	50 °C
2-HEAB + water									
0.0000		0.99704	0.98749	1.3325	1.3289	0.000	0.000	0.000	0.000
0.0293	1.676	1.03283	1.02016	1.3669	1.3623	-0.451	-0.418	123.698	126.878
0.0492	2.874	1.04701	1.03316	1.3819	1.3771	-0.652	-0.607	125.824	128.819
0.0745	4.470	1.05796	1.04396	1.3952	1.3914	-0.819	-0.783	128.089	130.645
0.1077	6.703	1.06746	1.05262	1.4096	1.4064	-0.991	-0.946	129.882	132.376
0.1532	10.049	1.07499	1.05877	1.4258	1.4205	-1.156	-1.079	131.536	134.115
0.2197	15.638	1.07803	1.06236	1.4373	1.4295	-1.213	-1.165	133.564	135.860
0.3255	26.807	1.07888	1.06332	1.4477	1.4421	-1.188	-1.159	135.435	137.602
0.5203	60.268	1.07753	1.06204	1.4579	1.4514	-0.978	-0.976	137.204	139.287
0.6145	88.550	1.07656	1.06112	1.4599	1.4535	-0.829	-0.841	137.735	139.794
0.7964	217.309	1.07514	1.05974	1.4638	1.4571	-0.530	-0.565	138.419	140.453
1.0000		1.07259	1.05680	1.4661	1.4590	0.000	0.000	0.000	0.000
2-HEAP + water									
0.0000		0.99704	0.98749	1.3325	1.3289	0.000	0.000	0.000	0.000
0.0122	0.6846	1.01150	1.00119	1.3478	1.3440	-0.195	-0.195	140.409	142.786
0.0270	1.5401	1.02437	1.01226	1.3626	1.3589	-0.390	-0.368	141.954	145.147
0.0453	2.6351	1.03465	1.02104	1.3782	1.3741	-0.566	-0.524	143.908	147.220
0.0683	4.0723	1.04207	1.02761	1.3905	1.3885	-0.712	-0.660	145.979	149.119
0.0996	6.1472	1.04746	1.03255	1.4018	1.4004	-0.841	-0.788	147.962	150.878
0.1422	9.2133	1.05108	1.03585	1.4126	1.4116	-0.956	-0.904	149.683	152.430
0.2045	14.2773	1.05298	1.03757	1.4245	1.4234	-1.049	-1.004	151.267	153.876
0.3060	24.4985	1.05331	1.03774	1.4358	1.4338	-1.113	-1.075	152.762	155.274
0.5000	55.5492	1.05162	1.03619	1.4477	1.4451	-1.069	-1.067	154.261	156.654
0.8608	343.5629	1.04651	1.03079	1.4630	1.4558	-0.500	-0.497	155.819	158.211
1.0000		1.04354	1.02785	1.4645	1.4561	0.000	0.000	0.000	0.000
2-HEAH + water									
0.0000		0.99704	0.98749	1..3325	1.3289	0.000	0.000	0.000	0.000
0.0111	0.6257	1.00891	0.99853	1.3478	1.3432	-0.189	-0.188	156.829	159.620
0.0250	1.4263	1.01923	1.00689	1.3617	1.3570	-0.380	-0.353	158.586	162.350
0.0418	2.4262	1.02614	1.01259	1.3748	1.3708	-0.534	-0.493	161.002	164.693
0.0636	3.7721	1.03093	1.01670	1.3877	1.3849	-0.673	-0.626	163.182	166.617
0.0921	5.6324	1.03450	1.01977	1.4002	1.3967	-0.819	-0.769	164.880	168.113
0.1330	8.5245	1.03698	1.02165	1.4132	1.4071	-0.982	-0.925	166.388	169.511
0.1937	13.3480	1.03806	1.02254	1.4247	1.4185	-1.162	-1.111	167.774	170.732
0.2899	22.6811	1.03728	1.02147	1.4354	1.4291	-1.339	-1.286	169.154	172.029
0.6782	84.6653	1.02532	1.00960	1.4576	1.4505	-0.777	-0.747	172.363	175.108
0.8773	397.3627	1.02137	1.00557	1.4618	1.4540	-0.264	-0.224	173.472	176.212
1.0000		1.01995	1.00438	1.4623	1.4548	0.000	0.000	0.000	0.000
2-HDEAH + water									
0.0000		0.99704	0.98749	1.3325	1.3289	0.000	0.000	0.000	0.000
0.0081	0.4551	1.01091	1.00056	1.3470	1.3434	-0.165	-0.168	188.682	192.109
0.0180	1.0157	1.02345	1.01133	1.3617	1.3573	-0.328	-0.314	190.753	195.319
0.0301	1.7250	1.03433	1.02060	1.3762	1.3724	-0.483	-0.452	192.993	197.789
0.0448	2.6085	1.04281	1.02818	1.3896	1.3849	-0.614	-0.580	195.339	199.871
0.0644	3.8219	1.05056	1.03526	1.4039	1.3998	-0.756	-0.725	197.279	201.537
0.0903	5.5124	1.05681	1.04094	1.4171	1.4135	-0.895	-0.870	199.115	203.164
0.1324	8.4767	1.06226	1.04593	1.4314	1.4279	-1.054	-1.044	201.066	204.909
0.1832	12.4630	1.06470	1.04810	1.4422	1.4379	-1.152	-1.164	202.738	206.444
0.4769	50.6553	1.06131	1.04449	1.4641	1.4567	-0.816	-0.961	207.318	210.783
1.0000		1.05871	1.03995	1.4714	1.4632	0.000	0.000	0.000	0.000

2-HEAH and 2-HDEAH, respectively. After these maximum values, the density starts to decrease, which can be observed more clearly for the hexanoate ionic liquids. The increase in density is possibly due to the increase in the ion-pair interactions between ionic liquid and water and the decrease in density can be due to the onset of self-interaction between the ions of the ionic liquid. The data in Table 2

show that the density values of the mixtures follow the order: 2-HEAB > 2-HDEAH > 2-HEAP > 2-HEAH, which indicates that the shorter alkyl chain of the cation is much denser than the lower alkyl chain (for example 1.072588 g.cm^{-3} for 2-HEAB and 1.058710 g.cm^{-3} for 2-HDEAH). This is due to the increase in dispersive interactions in ionic liquids with the increase in the chain length, resulting in a nano-structural organization in polar and nonpolar regions. As can be seen in Table 2, the hexanoate ionic liquids display significantly lower density values than the other ionic liquids (2-HEAB and 2-HEAP) due to the increased molecular mass of the anion. The temperature change did not lead to a significant behavior modification. Further analysis of Table 2 shows that the density decreases with increasing anion alkyl chain length (butanoate to hexanoate) and increases with decreasing cation alkyl chain length (diethylammonium to ethylammonium).

The experimental refractive index values for binary mixtures of ionic liquid + water are presented as function of ionic liquid mole fraction in Table 2, at 298.15 and 323.15 K. Differently from the density, the refractive index values increase with increasing composition of ionic liquid in the whole range studied. For the studied mixtures, the refractive index values followed the sequence 2-HDEAH > 2-HEAB > 2-HEAP > 2-HEAH. This order shows that hexanoate anion is present in the first and last positions, so this property seems to be more influenced by the cation. The highest refractive index values are due to the ion arrangement and the efficient packing of ions in the ionic liquids.

The refractive index values for binary mixtures of ionic liquids were also calculated using the Gladstone-Dale model (Rilo *et al*., 2012), Equation (1):

$$n_D = \phi_1 n_1 + \phi_2 n_2 \tag{1}$$

where ϕ_1 and ϕ_2 are the ionic liquid and water volume fractions, respectively, defined as:

$$\phi_1 = \frac{x_1 M_1 \rho_2}{x_1 M_1 \rho_2 + x_2 M_2 \rho_1} \tag{2}$$

$$\phi_2 = \frac{x_2 M_2 \rho_1}{x_1 M_1 \rho_2 + x_2 M_2 \rho_1} \tag{3}$$

For better investigation on the correlative capability of the proposed model the average absolute relative deviation (AARD%) and average relative deviation (ARD%) were verified, Equations (4) and (5).

$$AARD\% = \frac{100}{n}\sum_{i=1}^{n}\left|\frac{Y_{\exp} - Y_{calc}}{Y_{\exp}}\right| \tag{4}$$

$$ARD\% = \frac{100}{n}\sum_{i=1}^{n}\left(\frac{Y_{\exp} - Y_{calc}}{Y_{\exp}}\right) \tag{5}$$

where Y and n represent the property studied and the number of experimental data, espectively. As observed ion Table 3, calculated and experimental deviation values are very small for both temperature, increasing with temperature.

Table 3: Standard deviation from Equation (4), obtained by using the Gladstone-Dale model to reproduce values of the refractive index. T is temperature 298.15, 323.15 K.

	System	T/K	AARD%	ARD%
1	2-HEAB + water	298.15	0.562	0.562
2	2-HEAB + water	323.15	0.575	0.575
3	2-HEAP + water	298.15	0.153	0.147
4	2-HEAP + water	323.15	0.170	0.167
5	2-HEAH + water	298.15	0.431	0.431
6	2-HEAH + water	323.15	0.499	0.499
7	2-HDEAH + water	298.15	0.205	0.154
8	2-HDEAH + water	323.15	0.342	0.342

*Absolute Relative Deviation (AARD%) and Average Relative Deviation (ARD%).

Apparent Molar Volumes

The densities in Table 2 were used to calculate the apparent molar volumes using Equation (6):

$$V_{\phi,1} = \frac{M_1}{\rho} + \frac{1000}{m}\left(\frac{\rho_2 - \rho}{\rho\rho_2}\right) \tag{6}$$

where ρ and ρ_2 are the densities (g.cm^{-3}) of the solutions and water, respectively, M_1 is the molar mass of the ionic liquid, and m is the molality (mol.kg^{-1}) of the ionic liquid + water solution.

The values of apparent molar volumes, $V_{\phi,1}$, calculated with Equation (6), are listed in Table 2. The apparent molar properties reflect, more appropriately, interactions and structural changes induced by little added quantities of a second compound. The most significant change occurred in the water-rich region. After 0.3 ionic liquid molar fraction, the variation of $V_{\phi,1}$ is less apparent. The apparent molar volume followed the interaction order 2-HEAB > 2-HEAP > 2-HEAH > 2-HDEAH, at both temperatures studied. This order is inversely proportional to the compound molar mass, as can be observed in Table 2.

The limiting apparent molar volume, $V_{\phi,1}$, is the limiting volume that a substance occupies in one mole of other substance. In this limit, ions are surrounded only by the solvent, being infinitely distant from the other ions, and are unaffected by interaction among ions, so this is a pure measurement of the ion + solvent interaction (Wang *et al*., 2009; Patil *et al*., 2011). The apparent molar volume is calculated by fitting Equation (6), and fitted, as function of molality, to the Redlich-Meyer polynomial, Equation (7) (Alvarez *et al*., 2010b; De Oliveira *et al*., 2011):

$$V_{\phi,1} = V_{\phi}^{0} + S_v\sqrt{m} + B_V m \tag{7}$$

The slope, S_v, indicates the ion-ion interactions. For all systems at both temperatures, these parameters are positive, suggesting strong interactions between ion-solvent and ion-ion for the studied systems.

The parameters of Equation (7), V_{ϕ}^{0}, S_v and B_v and the average absolute relative deviation (AARD%) and average relative deviation (ARD%), defined by Equations (4) and (5), are presented in Table 4. The average relative deviation between the experimental and calculated value for all data points was less than 1.55%.

By observing the data of Table 4 it is possible to note that V_{ϕ}^{0} increases and S_v decreases as temperature increases. This indicates an increase in ion-solvent interactions and a decrease in ion-ion interactions with temperature.

Excess Molar Volumes

The excess molar volumes Vm^E are the sum of chemical, physical and structural effects of a mixture. Chemical interactions result in volume contraction, which include the charge transfer forces, forming or breaking complex forms of interaction. The contribution of the geometric adjustment is due to differences in molar volume and free volume between the components, giving a negative contribution to Vm^E.

The excess molar volumes Vm^E for binary systems were calculated according to Equation (8), and the resulting values are presented in Table 2.

$$Vm^E = \frac{x_1M_1 + x_2M_2}{\rho} - \frac{x_1M_1}{\rho_1} - \frac{x_2M_2}{\rho_2} \tag{8}$$

where x_1, ρ_1, and M_1 are the mole fraction, density, and molar masses of the pure ionic liquid, respectively, and x_2, ρ_2, and M_2 are the mole fraction, density, and molar masses of the water, respectively. The data for excess molar volume were correlated by the Redlich-Kister equation (Fan *et al*. 2008; Fan *et al*., 2009; Kurnia and Mutalib, 2011; Patil *et al*., 2011).

$$Vm^E = x_1x_2\Sigma A_k(x_1 - x_2)^k \tag{9}$$

where the coefficients A_k are parameters that were obtained by fitting the Redlich-Kister equation to the experimental values. The correlated results for excess volume are presented in Table 5, together with the average absolute relative deviation (AARD%) and average relative deviation (ARD%), defined by Equations (4) and (5). The average relative deviation between the experimental and calculated values for all data points was less than 6.81%.

Table 4: Coefficients of the Redlich-Meyer Equation for apparent molar volumes of ionic liquid + water at 298.15 and 323.15 K and AARD%. and ARD% as described below.

T/K	Ionic liquid	V_{ϕ}^{0}	S_v	B_v	AARD%	ARD%
298.15						
	2-HEAB	121.8068	3.198	-0.1453	0.786	0.019
	2-HEAP	140.9849	2.466	-0.094	1.014	0.261
	2-HEAH	157.8283	2.469	-0.086	0.915	0.143
	2-HDEAH	184.2724	7.506	-0.6042	1.547	1.547
323.15						
	2-HEAB	124.4482	3.121	-0.1430	0.702	0.102
	2-HEAP	144.1420	2.323	-0.088	0.998	0.245
	2-HEAH	161.3451	2.338	-0.081	0.871	0.130
	2-HDEAH	188.6344	7.409	-0.6097	1.260	1.260

*Absolute Relative Deviation (AARD%) and Average Relative Deviation (ARD%).

Table 5: Coefficients of the Redlich-Kister equation for Vm^E of ionic liquid + water at 298.15 and 323.15 K and AARD%. and ARD% as described below.

T/K		A_0	A_1	A_2	A_3	A_4	AARD%	ARD%
298.15								
	2-HEAB	-4.0130	2.5472	-2.1989	2.4546	-5.3203	1.945	0.286
	2-HEAP	-4.3775	1.7602	1.5687	1.7891	-9.5728	2.684	1.054
	2-HEAH	-5.1069	5.0288	5.2552	-1.4576	-11.6124	6.253	3.303
	2-HDEAH	-6.014	-72.909	-311.064	-440.245	-217.322	1.072	0.525
323.15								
	2-HEAB	-4.0298	2.1380	-2.0568	2.3012	-5.0591	1.815	-0.041
	2-HEAP	-4.4418	0.4555	0.5144	4.0960	-6.0846	3.932	2.122
	2-HEAH	-4.9917	4.9697	5.5745	-1.5412	-11.1148	6.813	3.578
	2-HDEAH	-6.984	-82.592	-340.987	-474.130	-228.818	1.766	1.107

*Absolute Relative Deviation (AARD%) and Average Relative Deviation (ARD%).

Figures 2 and 3, which depict the Vm^E plot of binary mixtures ionic liquids + water, show that the values are negative over a wide mole fraction range at 298.15 and 323.15 K under atmospheric pressure. The curves are asymmetric, with a *U*-shape for 2-HEAB and 2-HEAP and a *V*-shape for 2-HEAH and 2-HDEAH. The negative contribution arises from changes of the free volume in the real mixtures, comprising ions and water molecules; such behavior might arise from restriction of rotational motion, when the water molecules are accommodated interstitially within the ions.

Looking at the data in Figures 2 and 3, it is clear that the magnitude of the negative Vm^E values has a minimum at the mole fraction of ionic liquid ≈ 0.300 or ≈ 0.290 or ≈ 0.220 or ≈ 0.183 for 2-HEAP or 2-HEAH or 2-HEAB or 2-HDEAH, respectively. This indicates that the highest capacity packing occurs in these regions. This behavior can be attributed to the effect of packing and ion-dipole interactions of ionic liquids with water. Also from Figure 2, it can be noted that the magnitude of the Vm^E values showed the following trend at both temperatures, 298.15 and 323.15 K: 2-HEAH > 2-HEAB > 2-HDEAH > 2-HEAP. From this order it appears that the Vm^E magnitude is affected both by the cation and anion. The region of packing capacity decreased with the increase in the carbon chain length when the base is the same (2-HEAB > 2-HEAP) and when the acid is the same (2-HEAH > 2-HDEAH). Both changes make the Vm^E magnitude decrease with increasing alkyl chain length of the ionic liquid. Relative to the magnitude of Vm^E values, these values are quite close, with a low variation.

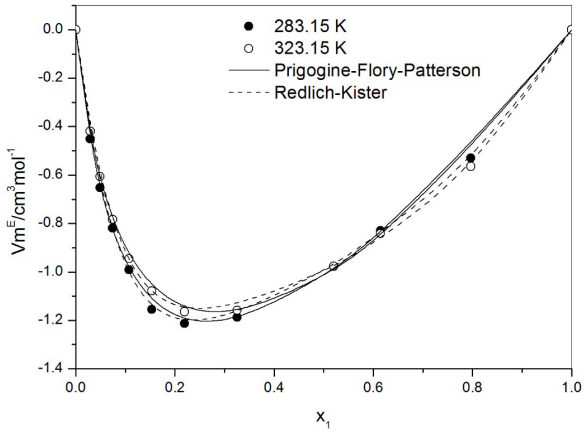

Figure 2: Plot of excess molar volumes against ionic liquid mole fraction (x_1) for 2-HEAB + water at T = 298.15 K (symbols) and T = 323.15 K; (line by models).

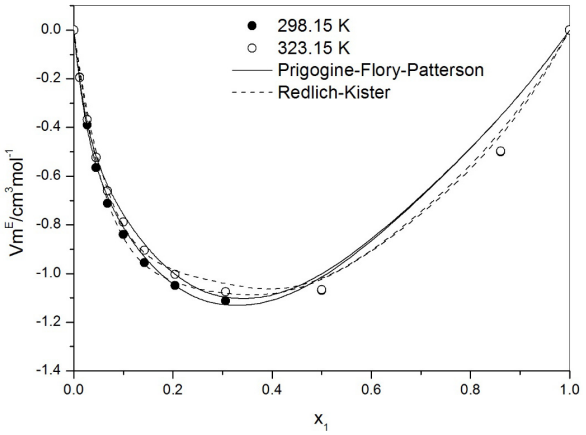

Figure 3: Plot of excess molar volumes against ionic liquid mole fraction (x_1) for 2-HEAP + water at T = 298.15 K (symbols) and T = 323.15 K; (line by models).

Prigogine-Flory-Patterson

The mixture density data, apparent molar volumes and excess molar volumes were modeled by the Prigogine-Flory-Patterson (PFP) theory (Prigogine, 1953; Prigogine, 1957; Flory and Orwoll, 1964[a,b]; Flory, 1965; Flory and Abe, 1965; Orwoll and Flory, 1967; Patterson, 1970; Costas and Patterson, 1982). This theory was extensively used to represent excess molar volume and enthalpy for various non-electrolytic liquid mixtures. According to the PFP theory, the excess molar volume Vm^E is divided into three contributions: (i) interactional, which is proportional to an empirical parameter, χ_{12}, called cross parameter, (ii) the free volume contribution, which arises from the dependence of the reduced volume on the reduced temperature as a result of the difference between the degree of expansion of the two components and (iii) the P^* contribution, which depends both on the differences of internal pressures and differences of reduced volumes of the components. PFP theory leads to the following expression for Vm^E in terms of the three contributions:

$$Vm^E = Vm^E{}_{\text{inter}} + Vm^E{}_{\text{free vol}} + Vm^E{}_{P*} \tag{10}$$

$$\frac{Vm^E}{\left(x_1V_1^* + x_2V_2^*\right)} = \frac{(\tilde{V}^{\frac{1}{3}} - 1)\tilde{V}^{\frac{2}{3}}\Psi_1\theta_2\chi_{12}}{\left(\left(\frac{4}{3}\right)\tilde{V}^{-\frac{1}{3}} - 1\right)P_1^*} - \frac{\left(\tilde{V}_1 - \tilde{V}_2\right)^2\left(\left(\frac{14}{9}\right)\tilde{V}^{-\frac{1}{3}} - 1\right)\Psi_1\Psi_2}{\left(\left(\frac{4}{3}\right)\tilde{V}^{-\frac{1}{3}} - 1\right)\tilde{V}} + \frac{(\tilde{V}_1 - \tilde{V}_2)(P_1^* - P_2^*)\Psi_1\Psi_2}{P_1^*\Psi_2 + P_2^*\Psi_1}$$

The $\tilde{V}$ of the solution is obtained through Flory's theory. The characteristic parameters V_i^* and P_i^* are obtained from the thermal expansion coefficient, α_i, and the isothermal compressibility, β_T. The thermal expansion coefficient is used to evaluate the reduced volume by the equation:

$$\tilde{V} = \Psi_1\tilde{V}_1 + \Psi_2\tilde{V}_2 \tag{11}$$

$$\tilde{V}_i = \left(\frac{1 + \left(\left(\frac{4}{3}\right)\alpha_i T\right)}{\left(1 + \alpha_i T\right)}\right)^3 \tag{12}$$

$$P_i^* = \frac{T\tilde{V}_i^{\,2}\,\alpha_i}{\beta_T} \tag{13}$$

Here, the molecular contact energy fraction is evaluated by:

$$\Psi_1 = 1 - \Psi_2 = \left(\frac{\varphi_1 P_1^*}{\varphi_1 P_1^* + \varphi_2 P_2^*}\right) \tag{14}$$

With the hard-core volume fractions defined by:

$$\phi_1 = 1 - \phi_2 = \frac{x_1 V_1^*}{(x_1 V_1^* + x_2 V_2^*)} \tag{15}$$

The values of the thermal expansion coefficient, α_i, the isothermal compressibility, β_T, as well as the interaction parameter, χ_{12}, were estimated using the experimental data.

The surface fractions are given by:

$$\theta_1 = 1 - \theta_2 = \frac{x_1 V_1^*\left(\frac{S_1}{S_2}\right)}{x_1 V_1^*\left(\frac{S_1}{S_2}\right) + x_2 V_2^*} \tag{16}$$

in which the ratio of the surface contact sites per segment is given by

$$\frac{S_1}{S_2} = \left(\frac{V_1^*}{V_2^*}\right)^{-1/3} \tag{17}$$

Parameter estimation problems involve estimating the unknown parameters of mathematical models based on a system of ordinary differential equations by using experimental data that are obtained under well-defined standard conditions. Traditional optimization methods such as the Nelder-Mead (NM) method (Nelder and Mead, 1965) and the Gauss-Newton method can be applied to find reasonably good estimations of parameters of simple models. However, they are not robust enough for complex

problems that involve a huge search space, and they tend to find local optimum points rather than the global optimum points. In addition, quasi-linearization methods and data-smoothing methods are also often used to solve parameter estimation problems (Yildirim *et al*. 2003).

The objective function used was a least-square objective function, as presented in Equation (18), considering deviations in the prediction of the excess volume.

$$Fobj = \sum_{i=1}^{N_{\exp}} \left(\left(y^{\exp} - y^{calc} \right)^2 \right) \quad (18)$$

Particle swarm optimization (PSO), developed by Kennedy and Eberhart (1995), is a stochastic global optimization technique inspired by social behavior of bird flocking or fish schooling. In the PSO, each particle in the swarm adjusts its position in the search space based on the best position it has found so far, as well as the position of the known best fit particle of the entire swarm, and finally converges to the global minimum of the whole search space. It should be mentioned that the objective function through the trial and error method was the average absolute relative deviation (AARD) combined with other statistical error analysis parameters, including the average relative deviation (ARD), for better investigation of the correlative capability of the proposed model (Schwaa and Pinto, 2007):

The estimated parameters for the PFP model are presented in Table 6 and the relative deviations are shown in Table 7.

Table 6: Estimated parameters α_i (K^{-1}), β_T (MPa^{-1}), χ_{12} ($J \cdot cm^{-3}$) for the PFP model and Vm ($cm^3.mol^{-1}$) molar volume of ionic liquid from experimental data.

	System	T/K	$10^3 \alpha_i$	$10^3 \beta_T$	χ_{12}	Vm
1	2-HEAB + water	298.15	1.92	2.92	-10.44	139.08
2	2-HEAB + water	323.15	1.78	2.58	-20.64	141.16
3	2-HDEAH + water	298.15	1.11	2.05	20.78	212.07
4	2-HDEAH + water	323.15	1.11	1.82	-0.39	215.30
5	2-HEAP + water	298.15	2.19	2.73	-45.60	156.40
6	2-HEAP + water	323.15	2.04	2.44	-56.14	158.79
7	2-HEAH + water	298.15	1.49	2.16	-25.25	173.77
8	2-HEAH + water	323.15	1.25	1.82	-25.92	176.47

Table 7: Systems used for modeling the Excess Molar Volume , Vm^E , and Apparent Molar Volumes, $V_{\phi,1}$, with the PFP model (Prigogine Flory Patterson). T is temperature, AARD% and ARD% are described below.

			Vm^E		$V_{\phi,1}$	
	System	T/K	AARD%	ARD%	AARD%	ARD%
1	2-HEAB + water	298.15	1.830	0.527	0.059	0.013
2	2-HEAB + water	323.15	2.331	0.545	0.085	0.032
3	2-HEAP + water	298.15	5.261	0.103	0.346	0.226
4	2-HEAP + water	323.15	4.829	0.404	0.279	0.174
5	2-HEAH + water	298.15	5.164	-1.088	0.254	-0.143
6	2-HEAH + water	323.15	7.260	-1.665	0.337	-0.218
7	2-HDEAH + water	298.15	3.051	1.535	0.296	-0.207
8	2-HDEAH + water	323.15	3.239	1.742	0.322	-0.234

*Absolute Relative Deviation (AARD%) and Average Relative Deviation (ARD%).

CONCLUSIONS

Four protic ionic liquids were synthesized by using several acids (butanoic, pentanoic and hexanoic) and bases (monoethanolamine and diethanolamine). Densities and refractive index of binary protic ionic liquid + water mixtures were measured at 298.15 K and 323.15K, under atmospheric pressure. The experimental density data of each mixture allowed the calculation of apparent and excess molar volumes. The Redlich-Meyer, Redlich-Kister and Prigogine-Flory-Patterson equations were used to fit the data.

The structures of the ionic liquids were confirmed by FT-IR analysis, where the four liquids showed salt charareristics, due to the presence of salt-specific bands. Density experimental results revealed that this property decreases with increasing anion alkyl chain length and increases with decreasing cation alkyl chain length. The density values for the mixtures studied increase as the concentration of the ionic liquid in water increases. This can be explained due to the increase in the ion-pair interactions between ionic liquid and water. In the ionic liquid-rich phase, the density smoothly decreases, due to the absence of these ion-pair interactions and the presence of self-interaction between the ions. The refractive index had a similar behavior, increasing with increasing ionic liquid composition, but never decreasing. On the contrary, in the ionic liquid-rich phase, the refractive index achieve a constant value. The highest refractive index values are due to the ion arrangement and to the efficient packing of ions. For the experimental refractive index, the cation influence is pretty clear. Interactions and structural characteristics, as well as apparent molar volumes, demonstrated that the most significant change occurred in the water-rich region. The apparent molar volume results were correlated with the Redlich-Meyer equation, while the excess volume data were correlated with the Redlich-Kister equation. The positive and high apparent molar volume values suggest strong ion-solvent interaction. The same interaction also becomes stronger as temperature increases. The apparent molar volume is the limiting volume that a substance occupies in one mole of the other substance; in this limit, ions are surrounded only by the solvent. The ionic liquid with the shortest carbon chains, 2-HEAB, yielded the lower apparent molar volumes, being the first to achieve this limiting condition. On the contrary, the ionic liquid with the longest carbon chains, 2-HDEAH, showed the highest apparent molar volumes, being the last to achieve the limiting condition, independent of cation or anion type. It also shows that strong ion-solvent interactions are directly linked to the carbon chain size. Excess volume values were negative and presented a smooth variation with increasing solute chain. Negative values indicate the packing efficiency ability or that attractive interactions occurred in ionic liquid + water solutions. The results proved to be useful for characterizing the influence of composition and temperature on the volumetric properties of mixtures (2-HEAB, 2-HEAP, 2-HEAH or 2-HDEAH + water) and also for understanding and interpreting the interactions that occurs during the process of mixing ionic liquid in water. For density and refractive index and also for the volumes, the most significant changes occurred in the water-rich region. In the ionic liquid-rich phase, the results showed a tendency to be constant, meaning a decrease in the ion-solvent interactions. The temperature variation has little influence on the results.

ACKNOWLEDGMENTS

We acknowledge the financial support from FAPESP (grant 2011/19736-1).

NOMECLATURE

$V_{\phi,1}$	apparent molar volume
Vm^E	excess molar volume
M_1	ionic liquid molar mass
x_1	ionic liquid mole fraction
V_ϕ^0	apparent molar volume at infinite dilution
m	Molality
Y_{calc}	number of calculated data
Y_{exp}	number of experimental data
n	parameters number
n_D	refractive index
M_2	water molar mass
x_2	water mole fraction

Greek Letters

ϕ_i	volume fraction
ρ	solution density
ρ_1	ionic liquid density
ρ_2	water density
σ	standard deviation

REFERENCES

Alvarez, V. H., Dosil, N., Gonzales-Cabaleiro, R., Mattedi, S., Martin-Pastor, M., Iglesias, M., Navaza, J. M., Brønsted ionic liquids for sustentable

process: Synthesis and physical properties. J. Chem. Eng. Data. 55, p. 625-632 (2010a).

Alvarez, V. H., Mattedi, S., Martin-Pastor, M., Aznar, M., Iglesias, M., Synthesis and thermophysical properties of two new protic long-chain ionic liquids with the oleate anion. Fluid Phase Equilib., 299, p. 42-50 (2010b).

Bicak, N., A new ionic liquid: 2-hydroxy ethylammonium formate. J. Mol. Liq., 116, p. 37-44 (2004).

Costas, M., Patterson, D., Volumes of mixing and the P* effect: Part II. Mixtures of alkanes with liquids of different internal pressures. J. Solution Chem., 11, p. 807-821 (1982).

Cota, I., Gonzalez-Olmos, R., Iglesias, M., Medina, F., New short aliphatic chain ionic liquids: Synthesis, physical properties, and catalytic activity in aldol condensations. J. Phys. Chem., B, 111, p. 12468-12477 (2007).

De Oliveira, L. H., Da Silva, J. L., Aznar, M., Apparent and partial molar volumes at infinite dilution and solid-liquid equilibria of dibenzothiophene + alkane systems. J. Chem. Eng., Data, 56, p. 3955-3962 (2011).

Fan, W., Zhou, Q., Zhang, S., Yan, R., Excess molar volume and viscosity deviation for the methanol + methyl methacrylate binary system at T = (283.15 to 333.15 K). J. Chem. Eng. Data, 53, p. 1836-1840 (2008).

Fan, W., Zhou, Q., Sun, J., Zhang, S., Density, excess molar volume, and viscosity for the methyl methacrylate + 1-butyl-3-methylimidazolium hexafluorophosphate ionic liquid binary system at atmospheric pressure. J. Chem. Eng. Data, 54, p. 2307-2311 (2009).

Flory, P. J., Abe, A., The thermodynamic properties of mixtures of small, nonpolar molecules. J. Am. Chem. Soc., 87, p. 1838-1846 (1965).

Flory, P. J., Statistical thermodynamics of liquid mixtures. J. Am. Chem. Soc., 87, p. 1833-1838 (1965).

Flory, P. J., Orwoll, R. A., Vrij, A., Statistical thermodynamics of chain molecule liquids. II. Liquid mixtures of normal paraffin hydrocarbons. J. Am. Chem. Soc. 86, p. 3515-3520 (1964a).

Flory, P. J., Orwoll, R. A., Vrij, A., Statistical thermodynamics of chain molecule liquids. I. An equation of state for normal paraffin hydrocarbons. J. Am. Chem. Soc., 86, p. 3507-3515 (1964b).

Iglesias, M., Torres, A., Gonzales-Olmos, R., Salvatierra, D., Effect of temperature on mixing thermodynamics of a new ionic liquid: {2-hidroxy ethylammoniumformate (2-HEAF) + short hydroxylic solvents}. J. Chem. Thermodyn. 40, p. 119-133 (2008).

Iglesias, M., Gonzales-Olmos, R., Cota, I., Medina, F., Brønsted ionic liquids: Study of physicochemical properties and catalytic activity in aldol condensations. Chem. Eng. J., 162, p. 802-808 (2010).

Kapadi, U. R., Hundiwale, D. G., Patil, N. B., Lande, M. K., Viscosities, excess molar volume of binary mixtures of ethanolamine with water at 303.15, 308.15, 313.15 and 318.15 K. Fluid Phase Equilib., 201, p. 335-341 (2002).

Kennedy, J., Eberhart, R., "Particle Swarm Optimization". In: Proceedings of IEEE International Conference on Neural Networks IV: 1942-1948, Perth, WA, Nov/Dec (1995).

Kurnia, K. A., Mutalib, M. I. A., Densities and viscosities of binary mixture of the ionic liquids bis (2-hydroxyethil) ammonium propionate with methanol, ethanol, and 1-propanol at T=(293.15, 303.15, 313.15 and 323.15) K and at P= 0.1 MPa. J. Chem. Eng. Data, 56, p. 79-83 (2011).

Nelder, J. A., Mead, R., A Simplex method for function minimization. Computer J., 7, p. 308-313 (1965).

Orwoll, R., Flory, P. J., Equation-of-state parameters for normal alkanes. Correlation with chain length. J. Am. Chem. Soc., 89, p. 6814-6822 (1967).

Patil, P. P., Patil, S. R., Borse, A. U., Hundiwale, D. G., Density, excess molar volume and apparent molar volume of binary liquid mixtures. Rasayan J. Chem., 4, p. 599-604 (2011).

Patterson, D., Delmas, G., Corresponding states theories and liquid models. Discuss. Faraday Soc., 49, p. 98-105 (1970).

Prigogine, I., The Molecular Theory of Solutions. North Holland, Amsterdam (1957).

Prigogine, I., Trappeniers, N., Mathot, V., Statistical thermodynamics of r-MERS and r-MER solutions. Discuss. Faraday Soc., 15, p. 93-107 (1953).

Rilo, E., Domínguez-Pérez, M., Vila, J., Segade, L., García, M., Varela, L. M., Cabeza, O., Easy prediction of the refractive index for binary mixtures of ionic liquids with water or ethanol. J. Chem. Thermodyn., 47, 219-222 (2012).

Schwaab, M., Pinto, J. C., Análise de Dados Experimentais I: Fundamentos de Estatística e Estimação de Parâmetros, Rio de Janeiro, e-papers (2007). (In Portuguese).

Taib, M. M., Ziyada, A. K., Wilfred, C. D., Murugesan, T., Volumetric properties and refractive indices for binary mistures of 1-propyronitrile-3-hexylimidazolium bromide + ethanol at temperatures from 293.15 to 323.15 K. J. Sol. Chem., 41, p. 100-111 (2012).

Wang, J., Zhang, S., Wang, H., Pei, Y., Apparent molar volumes and electrical conductance of ionic liquids [$C_n$min]Br dimethylsulfoxide at 298.15 K. J. Chem. Eng. Data, 54, p. 3252-3258 (2009).

Yildirim, N., Akcay, F., Okur, H., Yildirim, D., Parameter estimation of nonlinear models in biochemistry: A comparative study on optimization methods. Appl. Math. Comput., 140, p. 29-36 (2003).